Journal of Associated Medical Sciences 2025; 58(3): 173-183

JAMS
Journal of Associated Medical Sciences

Scopus Indexed & Thai-Journal Citation Index Centre (TCI)

Journal of Associated Medical Sciences

Journal homepage: https://www.tci-thaijo.org/index.php/bulletinAMS/index

The preparation of Au decorated on ZnO nanorods by comparative DCMS/HIPIMS techniques for antibacterial activity

Sukon Kalasung[1], Saksorn Limwichean[2], Pitak Eiamchai[2], Mati Horprathum[2], Noppadon Nuntawong[2], Viyapol Patthanasettakul[2], Artitaya Yatsomboon[1*]

[1]Faculty of Medicine, Bangkokthonburi University, Thawi Watthana, Bangkok, Thailand.
[2]National Electronics and Computer Technology Center, National Science and Development Agency, Pathum Thani, Thailand.

ARTICLE INFO

Article history:
Received 7 February 2025
Accepted as revised 29 May 2025
Available online 27 June 2025

Keywords:
Au-decorated ZnO NRs, hybrid nanomaterials, novel antimicrobial agents, Escherichia coli, Staphylococcus aureus.

ABSTRACT

Background: The mortality rate of antimicrobial-resistant infections has increased dramatically worldwide due to the increased use of antibiotics. The rise of antibiotic-resistant bacteria has highlighted the need to develop novel materials with antimicrobial properties, and nanotechnology offers promising prospects for the development of new therapeutic approaches. Currently, hybrid nanomaterials are interesting alternatives that enhance the physical and antibacterial properties of nanomaterials with a large surface area, making them efficient and biocompatible.

Objectives: This study evaluated the antibacterial activity of Au nanoparticle-decorated ZnO Nanorods (NRs) with different characteristics of Au nanoparticles (Au NPs) on the ZnO surface.

Materials and methods: ZnO NRs were grown on a silicon wafer using the hydrothermal method, and Au NPs were decorated on the ZnO NRs surface by DC magnetron sputtering and high-power impulse magnetron sputtering (HiPIMS) techniques for comparison. The physical morphologies and crystallinity of the ZnO NRs and Au-nanoparticle-decorated ZnO NRs were investigated by field-emission electron microscopy (FE-SEM), transmission electron microscopy (TEM), and X-ray diffraction (XRD).

Results: FE-SEM results indicated changes in the physical morphologies of the Au NPs on the ZnO NRs. The antibacterial efficacy of the ZnO NRs and Au-decorated ZnO NRs against *Escherichia coli* and *Staphylococcus aureus* was evaluated under UV light irradiation with bacterial concentrations ranging from 10^0 to 10^8 CFU/mL to assess their inhibitory effects using the plate count technique.

Conclusion: The results demonstrated that the proposed Au-ZnO NRs exhibited a significant inhibitory effect on the growth of *Escherichia coli* indicating the potential of Au NPs decorated ZnO NRs as a novel antimicrobial material. Importantly, the results highlight the influence of bacterial concentration on the effectiveness of Au-ZnO NRs, offering insights for future applications in combating antibiotic-resistant bacteria.

Introduction

Antimicrobial resistance (AMR) is an escalating global health issue, characterized by the diminishing efficacy of antibiotics against bacterial pathogens. This crisis, driven by the overuse and misuse of antimicrobial agents, poses severe threats to healthcare systems, agriculture, and global economy. The World Health Organization (WHO) has projected that, by 2050, AMR-related infections could result in 10 million deaths annually, surpassing cancer and cardiovascular diseases as the leading causes of mortality.[1,2] The rapid emergence of resistant strains

∗ **Corresponding contributor.**
Author's Address: *Faculty of Medicine, Bangkokthonburi University, Thawi Watthana, Bangkok, Thailand.*
E-mail address: artitaya.yat@bkkthon.ac.th
doi: 10.12982/JAMS.2025.086
E-ISSN: 2539-6056

of bacteria, such as *Escherichia coli* and *Staphylococcus aureus*, underscores the urgent need for innovative strategies to manage bacterial infections. Nanotechnology offers promising solutions for AMR by leveraging the unique properties of nanoscale materials. Zinc oxide nanorods (ZnO NRs) are among the most studied nanomaterials for their intrinsic antibacterial activity, which is attributed to the generation of reactive oxygen species (ROS) and the release of zinc ions that disrupt bacterial membranes and DNA.[3] Hybrid nanostructures, such as gold nanoparticle (AuNP)-decorated ZnO NRs, have shown synergistic effects that enhance antimicrobial efficacy.[4] The addition of AuNPs amplifies ROS production through plasmonic effects and provides additional antibacterial mechanisms, such as ion release and physical damage to bacterial cell walls.[5] Recent studies have explored various synthesis techniques for Au-ZnO hybrid nanomaterials. Among these, sputtering methods, including direct current magnetron sputtering (DCMS) and high-power impulse magnetron sputtering (HIPIMS), have been widely used because of their ability to produce uniform coatings and control particle size.[6] HIPIMS, in particular, offers high-energy pulsed deposition, resulting in superior nanoparticle distribution and enhanced antibacterial properties compared to traditional methods. Despite these advancements, the comparative efficacy of Au-ZnO NRs fabricated by DCMS and HIPIMS remains underexplored, particularly in terms of their performance against clinically relevant pathogens, such as *E. coli* and *S. aureus.*[7] While significant progress has been made in developing ZnO-based nanostructures, several gaps remain.[8] The influence of fabrication techniques on the physical, chemical, and antibacterial properties of Au-ZnO NRs is not fully understood. Furthermore, there is limited knowledge of the optimal conditions for enhancing the performance of these materials under UVA light exposure, which is a critical factor in their potential applications in healthcare and environmental settings. Addressing these gaps is essential for advancing the practical use of hybrid nanomaterials to combat AMR.

This study aimed to investigate the preparation and antibacterial efficacy of Au-decorated ZnO NRs fabricated using the DCMS and HIPIMS techniques. The specific objectives were 1) to compare the physical and structural properties of Au-ZnO NRs synthesized using DCMS and HIPIMS, 2) to evaluate their antibacterial performance against *E. coli* and *S. aureus* under UVA exposure, and 3) to identify the production conditions that maximize antibacterial efficacy. The significance of this study lies in its potential to provide a scientific basis for optimizing the design and production of hybrid nanomaterials. By addressing the challenges associated with AMR, this study contributes to the development of effective antimicrobial agents that can be integrated into medical devices, water treatment systems, and other critical applications.

Materials and methods

Materials

The bacterial strains used in this study were *Escherichia coli* (ATCC 25922) and *Staphylococcus aureus* (ATCC 29213). The culture medium used for bacterial growth and experimentation consisted of Nutrient Broth (NB; Difco, USA) and Nutrient Agar (NA; Oxoid, UK). Reagents and solutions included Normal Saline Solution (0.9% NaCl; Sigma-Aldrich, USA) and the McFarland Standard 0.5 (0.5; Remel, USA) for bacterial standardization. The equipment used included a UV-A light source (220 W; Philips, Netherlands), an incubator set at 37 °C (Thermo Fisher Scientific, USA), a densitometer DEN-2 model (Biosan, Latvia) for turbidity measurement, and a plate counter for bacterial colony enumeration. Zinc nitrate hexahydrate ($Zn(NO_3)_2 \cdot 6H_2O$, 98%) was purchased from Laboratory Reagent & Fine Chemical (LOBA Chemie). HMTA ($C_6H_{12}N_4$, ≥99.0%) was purchased from Sigma-Aldrich (St. Louis, MO, USA). A Zn sputtering target (2-inch diameter and 99.99 % purity) was purchased from Kurt J. Lesker (Pennsylvania, USA). A gold (Au) sputtering target (2-inch diameter and 96.5% purity) was obtained from Siam Gold Gallery Co., Ltd. (Thailand).

Preparation of the Au nanoparticles-decorated ZnO NRs

Au-decorated ZnO nanorods were fabricated using a multistep process, as illustrated in Figure 1. First, 100 nm ZnO films on 2×4 cm^2 n-type silicon (100) wafers were used as base substrates. These films were prepared via DC magnetron sputtering using a Zn target operated at 100 W with argon and oxygen flow rates of 20 and 40 sccm, respectively. Next, the base substrates were immersed in a mixed solution of zinc nitrate hexahydrate and HMTA at a 1:1 ratio in 200 ml of deionized (DI) water at a concentration of 10 mM. For the hydrothermal synthesis, the solution-containing substrates were transferred to an autoclave set at 90 °C for 4 hrs. The hydrothermally grown ZnO NRs arrays were carefully removed, rinsed, and dried under ambient air. Finally, the prepared ZnO NR templates were decorated with Au nanoparticles using pulsed DC magnetron sputtering (DCMS) at 100 W, 5 mTorr operating pressure, and a 20 sccm argon flow rate for deposition times of 15 sec and 60 sec. High-power impulse magnetron sputtering (HiPIMS) was employed, with a pulse width of 100 µs, frequency of 700 Hz, 5 mTorr operating pressure, and 20 sccm argon flow rate for deposition times of 15 sec and 60 sec (AJA International, Inc.; ATC 2000-F). In this study, Au NPs were decorated on ZnO NR surfaces using a comparative DCMS and HiPIMS approach to investigate their antibacterial activity.

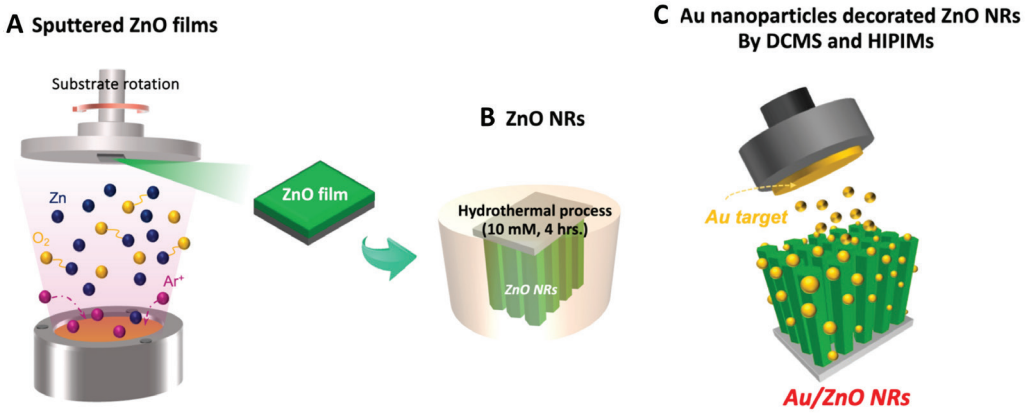

Figure 1. *Preparation procedure for design of Au-nanoparticles decorated ZnO nanorods.*

Characterization of the Au nanoparticles -decorated ZnO nanorods

The physical morphologies of the fabricated samples were analyzed using field-emission scanning electron microscopy (FE-SEM; Hitachi High Tech; SU8030) at an accelerating voltage of 10 kV. Top-view and cross-sectional FE-SEM images were captured for both the ZnO NRs and Au-nanoparticle decorated ZnO NRs, with measurements such as diameter and height taken at up to 50 positions for each sample. The crystallinity of the ZnO NRs and Au-decorated ZnO NRs was investigated using X-ray diffraction (XRD). Further analyses of the physical morphologies and elemental/compound compositions were performed on a single Au-decorated ZnO NRs sample. These nanorods were carefully scraped onto copper grids and examined using a transmission electron microscope (TEM; JEOL, JEM-2100 Plus) operated at an accelerating voltage of 200 kV. Additionally, Energy-dispersive X-ray spectroscopy (EDS) was performed to map the elemental distribution of Au, Zn, and O. Finally, high-resolution TEM (HR-TEM) imaging and selected area electron diffraction (SAED) were carried out specifically on the topmost and central regions of the selected Au-decorated ZnO nanorods.

Antibacterial Test

The antibacterial activity of the Au-decorated ZnO nanorods (Au-ZnO NRs) was evaluated against *Escherichia coli* and *Staphylococcus aureus* under UV-A exposure. Both bacterial strains were first cultured in 3mL of Nutrient Broth (NB) at 37 °C with shaking at 150 rpm for 18-24 hrs to reach the exponential growth phase. The bacterial suspensions were then standardized to the McFarland 0.5 turbidity standard, corresponding to approximately 1.5×10^8 CFU/mL, using a densitometer. Serial dilutions were subsequently performed using sterile saline or NB to achieve bacterial concentrations ranging from 10 CFU/mL to 10 CFU/mL. For antibacterial testing, sterilized Au-ZnO NR samples were placed in sterile Petri dishes (five samples per dish), and 100µL of bacterial suspension was applied to each sample. The dishes were exposed to UV-A light (220 W) for 1 hr at a fixed distance to ensure consistent irradiation. Control groups containing bacterial suspensions without nanorods were subjected to the same UV-A exposure conditions. After treatment, all samples were incubated at 37 °C for 18–24 hrs to allow the surviving bacteria to form visible colonies. The number of colony-forming units (CFUs) was counted using the plate count method, and antibacterial efficacy was determined by calculating the Killing Rate using the following formula:

$$\text{Killing rate (\%)} = [(\text{CFU\_control} - \text{CFU\_treated}) / \text{CFU\_control}] \times 100.$$

Statistical analysis

The experimental results are expressed as the mean ± standard deviation. Statistical significance was analyzed using one-way ANOVA, followed by post-hoc tests to compare multiple groups. Statistical significance was set at $p<0.05$. All experiments were performed in triplicate to ensure reproducibility and minimize variability.

Results

Figure 2A presents the top-view and cross-sectional FE-SEM images of the ZnO NRs and Au-decorated ZnO NRs, along with histograms illustrating the distribution of the NR diameters and lengths measured from a sample size of 2 mm^2. Figure 2B displays the Gaussian-fitted distributions of (i) the diameters and (ii) lengths of the ZnO NRs and Au-decorated ZnO NRs. The average diameter was approximately 120 nm, with a standard deviation (SD) of 30 nm, while the average length was approximately 2,221 nm, with an SD of 46 nm. Figure 3A clearly shows the morphology of the Au nanoparticles deposited on the surface of the ZnO NRs. Figure 3B Additionally, after Au deposition, the samples were examined using X-ray diffraction (XRD) to confirm the presence of Au nanoparticles on the ZnO NR surfaces. The XRD patterns of the ZnO NRs exhibited diffraction peaks corresponding to the wurtzite structure, with prominent peaks observed at 34.8°, 45.7°, and 63.2°, which were indexed to the (002), (102), and (103) planes of ZnO, respectively. (JCPDS card No. 01-070-8072).

After Au decoration, an additional diffraction peak appeared at 38.272°, corresponding to the (111) crystallographic plane of face-centered cubic (FCC) Au (JCPDS card No. 04-004-8456), confirming the successful deposition of Au nanoparticles. This result indicates that the Au nanoparticles exhibit a strong preferential (111) orientation,[4,9-11] suggesting a highly ordered and textured

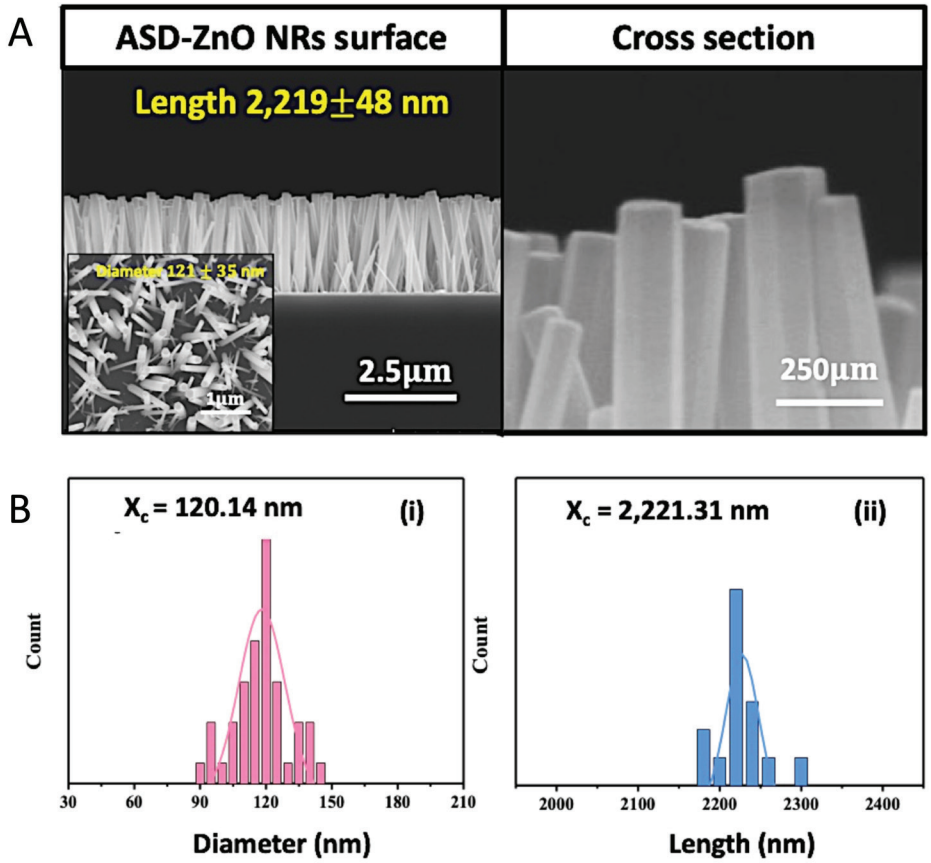

Figure 2. *Morphological and dimensional characterization of ASD-ZnO nanorods (NRs). A: FE-SEM image showing the physical morphologies of ASD-ZnO NRs, B: corresponding distribution plots of the diameter (pink) and length (blue) of the ZnO NRs templates.*

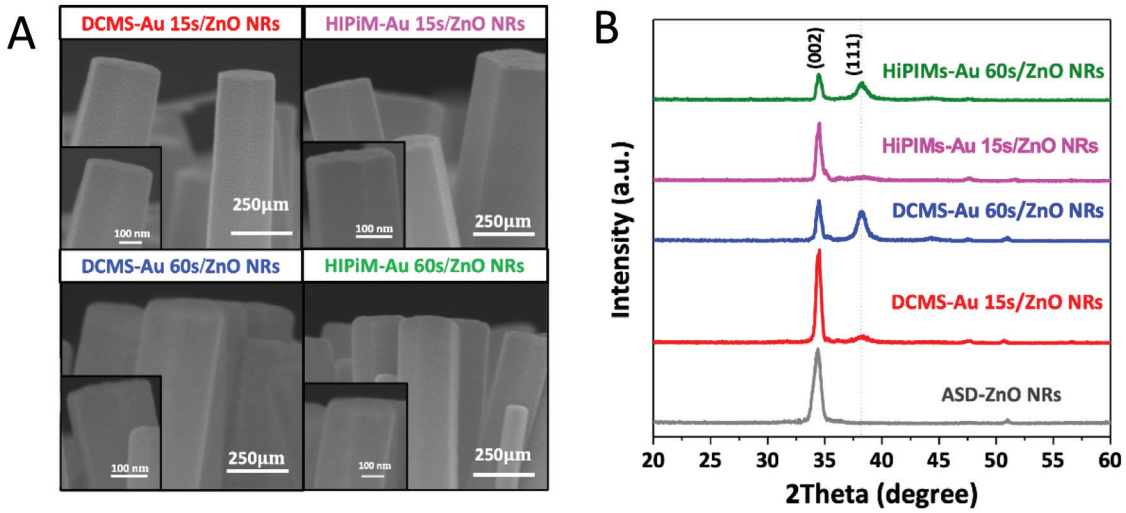

Figure 3. *Surface morphology and crystal structure of Au-decorated ZnO nanorods (NRs) prepared by DCMS and HiPIMS techniques. A: FE-SEM images showing the surface morphologies of Au-decorated ZnO NRs fabricated using DCMS and HiPIMS techniques at different Au deposition times (15 and 60 sec). Distinct differences in the distribution of Au nanoparticles were clearly observed. Red, blue, pink, and green text annotations indicate DCMS-Au 15 sec/ZnO NRs, DCMS-Au 60 sec/ZnO NRs, HiPIMS-Au 15 sec/ZnO NRs, and HiPIMS-Au 60 sec/ZnO NRs, respectively, B: XRD patterns of ZnO NRs and Au-decorated ZnO NRs prepared using the DCMS and HiPIMS techniques are shown. The gray line corresponds to the ZnO NRs, with diffraction peaks at 34.8°, 45.7°, and 63.2°. After Au deposition, an additional diffraction peak was observed at 38.272°. Red, blue, pink, and green lines represent the DCMS-Au 15 sec/ZnO NRs, DCMS-Au 60 sec/ZnO NRs, HIPIMS-Au 15 sec/ZnO NRs, and HIPIMS-Au 60 sec/ZnO NRs, respectively.*

structure. The preferential (111) growth of Au is expected to enhance the surface reactivity of Au-ZnO NRs.

To provide clearer evidence of how the gold nanoparticle morphology on the ZnO NRs surface varies with different deposition times (15 and 60 sec) and to support a more robust structural interpretation, we have included additional analysis beyond the FE-SEM images shown in Figure 3a), which has limitations and does not clearly reveal the presence or distribution of gold on the ZnO surface. Additional TEM images of the DCMS-Au 15 sec/ZnO NRs and DCMS-Au 60 sec/ZnO NRs samples are shown in Figure 4. Figure 4A illustrates the morphology of the Au-decorated ZnO nanorods after 15 sec of gold deposition, in which discrete Au nanoparticles were uniformly distributed over the nanorod surface. In contrast, Figure 4B (60 sec deposition) clearly shows a significant coalescence of Au nanoparticles, forming a continuous on the nanorod surfaces.

Furthermore, high-magnification TEM images at 1,000,000×, shown in Figure 4A and 4B for DCMS-Au 15 sec/ZnO NRs and DCMS-Au 60 sec/ZnO NRs, respectively, clearly reveal the crystalline structure of the AuNPs deposited on the ZnO NRs. In particular, the inset (i) displays distinct lattice fringes corresponding to the gold crystallites. These observations were further supported by elemental analysis via EDX mapping. As shown in Figure 5A, for the 15 sec Au-deposited sample, EDX elemental maps clearly illustrate the spatial distribution of gold (red; l), oxygen (blue; m), and zinc (green; n). Gold nanoparticles were observed as discrete, well-dispersed spots on the ZnO NR surfaces, consistent with the particle-like morphology observed in the corresponding TEM inset (i). In contrast, Figure 5B shows a significant morphological transformation for the 60 sec Au-deposited sample. The EDX map reveals a continuous gold (red; l) film covering the ZnO nanorod surfaces, as corroborated by inset (i) of the TEM image. This indicates substantial nanoparticle coalescence and film formation as a function of increased deposition time. These results confirm the morphological transition of Au as a function of deposition time.

The antibacterial efficacies of ZnO NRs and Au-ZnO NRs were evaluated. From figure 6A the antibacterial performance of ZnO NRs and Au-ZnO NRs was assessed against *Escherichia coli* at an initial concentration of 10^6 CFU/mL under UV-A exposure for 1 hr. The results revealed significant variations in bacterial inhibition depending on sputtering technique and deposition duration. ASD-ZnO NRs exhibited the lowest antibacterial efficiency (Figure 6B), with a killing rate of 26.64%, indicating limited antibacterial activity. In contrast, Au-ZnO NRs demonstrated enhanced antibacterial efficacy. Among the samples, the HiPIMS-Au 15 sec condition achieved the highest bacterial reduction of 99.62%, highlighting the superior antibacterial effect of the HiPIMS sputtering. Other Au-decorated samples, such as HiPIMS-Au 60 sec (89.62%), DCMS-Au 15 sec (85.69%), and DCMS-Au 60 sec (84.93%), also exhibited significant bacterial reduction compared to the control. These findings indicate that both the sputtering technique and the deposition duration play crucial roles in determining the antibacterial efficacy of Au-ZnO NRs.

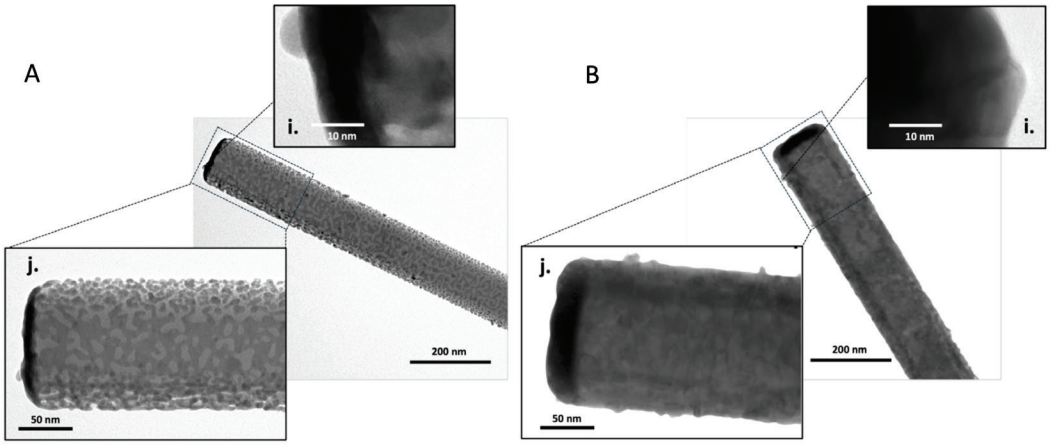

Figure 4. *High-resolution TEM images of a single Au-decorated ZnO nanorod fabricated using DCMS at two deposition times. A: 15 sec, B: 60 sec, i: insets clearly show lattice fringes corresponding to crystalline Au, confirming the presence of AuNPs on ZnO NRs.*

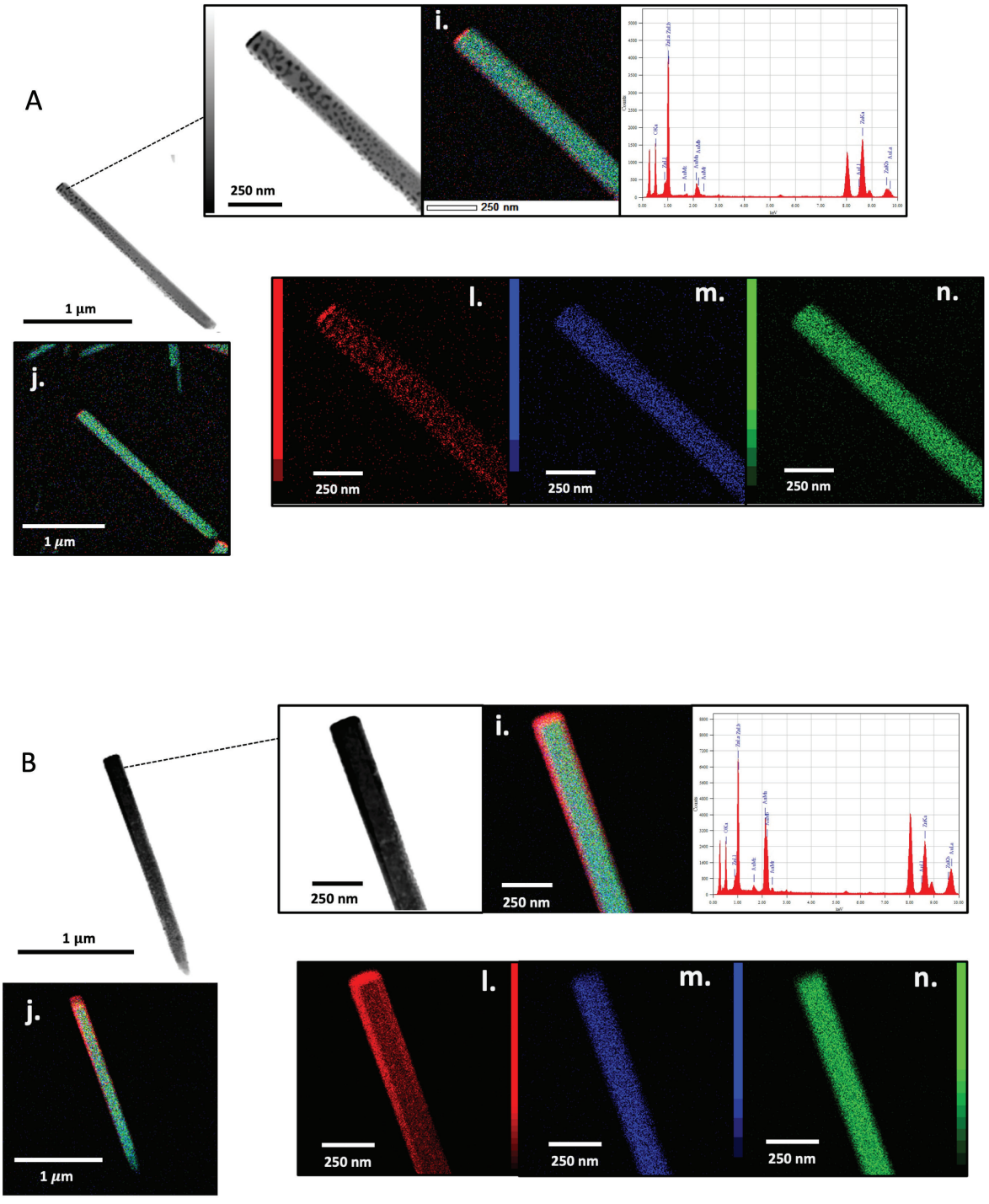

Figure 5. *EDX elemental mapping of a single Au-decorated ZnO nanorod. A: DCMS-Au 15 sec; B: DCMS-Au 60 sec. The elemental distributions of Au (red, l), O (blue, m), and Zn (green, n) are presented. For the 15 sec sample, Au appears as dispersed nanoparticles on the ZnO nanorods, as shown in Figure 5A (i, j), whereas for the 60 sec sample, Au forms a continuous film coating the nanorods, as shown as Figure 5B (I, j).*

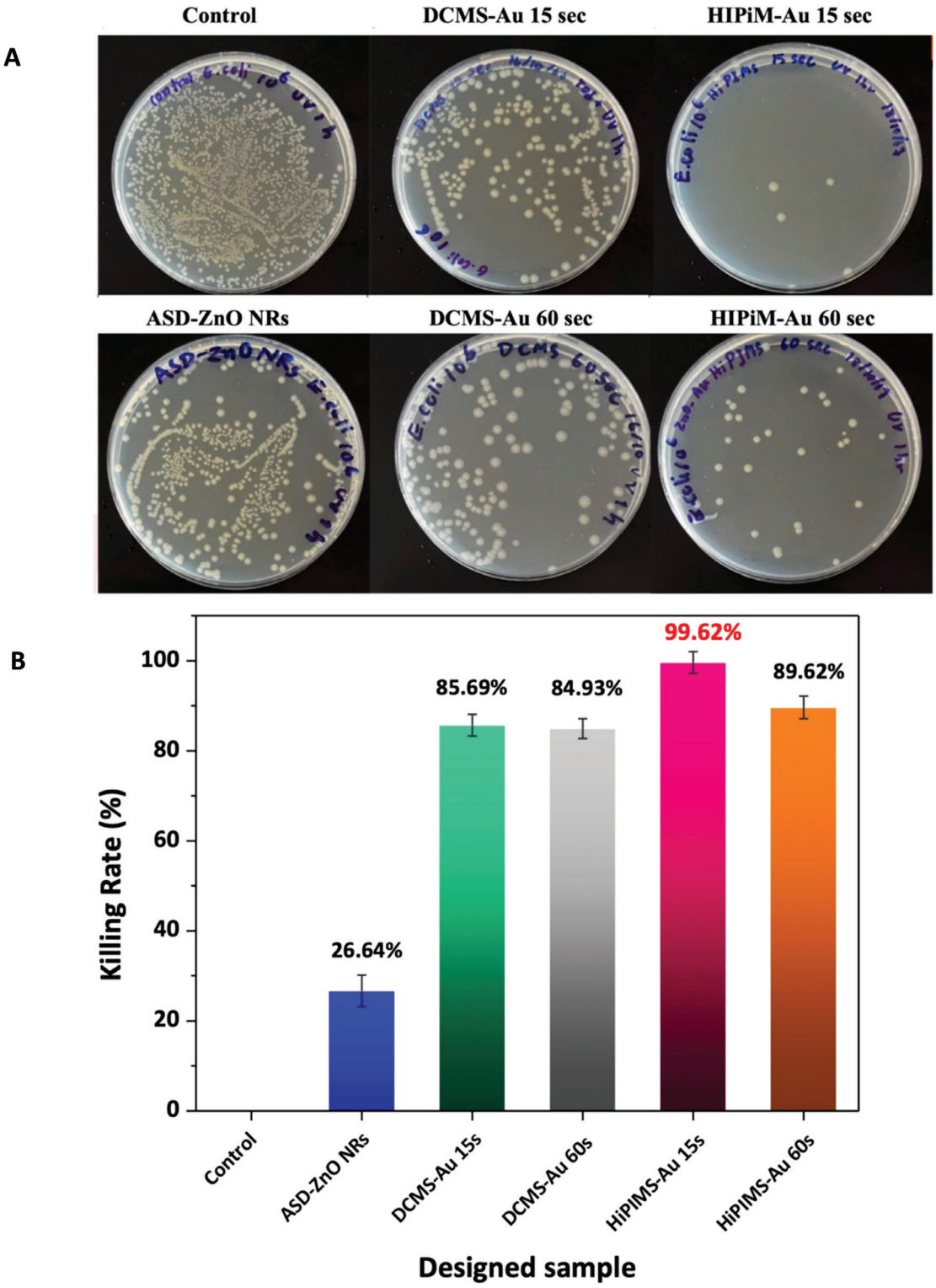

Figure 6. *Comparative antibacterial efficacy of ZnO nanorods and Au-decorated ZnO nanorods fabricated by DCMS and HiPIMS techniques under UV-A exposure. A: antibacterial efficacy of ZnO and Au-ZnO NRs was evaluated against Escherichia coli at a concentration of 10^6 CFU/mL under UV-A exposure for 1 hr. The results demonstrate significant variations in antibacterial activity based on the sputtering technique and duration. B: antibacterial killing rate of ZnO NRs and Au-ZnO NRs against Escherichia coli under UV-A exposure.*

Discussion

Figure 2A shows significant changes in the physical morphology of the NRs before and after the Au decoration process. The ZnO NRs exhibited a hexagonal structure with uniform distribution across the surface of the sample. As shown in Figure 3A, at a deposition time of 15 sec, the Au nanoparticles appeared as small, isolated particles. When the deposition time was increased to 60 sec, the Au nanoparticles formed an island-like structure that covered the entire surface of the NRs. The FE-SEM and TEM images clearly show the presence of Au nanoparticles coated on the ZnO NRs, compared to the FE-SEM images before Au deposition, as shown in Figure 2A and Figure 4, respectively. Figure 3B clearly shows a strong peak (002), which corresponds to the preferred ZnO growth direction along the c-axis. The other diffraction peak at 38.2°, corresponding to the (111) plane, was indexed as Au. From the antibacterial efficacy testing of the ZnO NRs and Au-ZnO NRs, the untreated control samples exhibited dense bacterial colonies, indicating no reduction in bacterial growth (Figure 6a, top left). This confirmed that UV-A exposure alone did not significantly inhibit bacterial survival. ASD-ZnO NRs (Pure ZnO): The ZnO NRs without Au decoration showed limited antibacterial activity, achieving a killing rate of 26.64% (Figure 6B).

This reflects the inherent but insufficient antibacterial properties of ZnO, which can generate reactive oxygen species (ROS), but not at levels sufficient to eradicate high bacterial loads. DCMS-decorated Au-ZnO NRs: Au-ZnO NRs prepared via DCMS sputtering for 15 sec demonstrated a killing rate of 85.69% (Figure 6A), top middle, and Figure 6B, representing a significant enhancement compared with pure ZnO NRs. Extending the sputtering time to 60 sec yielded a slightly lower killing rate of 84.93%, possibly because of nanoparticle aggregation, which reduced the effective surface area for bacterial interaction and ROS generation. This hypothesis is strongly supported by the high-resolution TEM and EDX mapping analyses presented in Figures 4 Figure 5 illustrates the morphology of Au-decorated ZnO NRs after 15 sec of gold deposition, where discrete Au nanoparticles are uniformly distributed across the NR surface. In contrast, Figure 4B (60 sec deposition) clearly reveals significant nanoparticle coalescence, resulting in a continuous film-like coverage of Au on the ZnO surface. This morphological transformation can be explained by the classical nucleation and growth theory. At shorter deposition times, the limited atomic flux and surface diffusion favor the formation of discrete nanoclusters. As the deposition time increased, the surface accumulated Au atoms, enhancing surface diffusion and promoting coalescence through grain-boundary migration mechanisms. This results in larger aggregates or film-like structures that reduce the specific surface area and limit effective bacterium-nanomaterial interactions. Furthermore, EDX elemental mapping supported this observation. For the 15 sec, sample gold was clearly seen as isolated (Figure 5A), well-dispersed nanoparticles, while the 60 sec sample (Figure 5B) revealed a near-continuous gold layer enveloping the ZnO nanorods. These findings provide quantitative and visual confirmation that extended deposition time promotes nanoparticle aggregation, which, in turn, diminishes antibacterial efficacy.

Taken together, the TEM and EDX mapping data corroborate the observed decline in the bacterial killing rate at 60 sec and validate the mechanistic hypothesis that nanoparticle aggregation negatively impacts antibacterial performance.

HIPIMS-decorated Au-ZnO NRs: HiPIMS sputtering for 15 sec achieved the highest antibacterial efficacy, with a killing rate of 99.62% (Figure 6A), top right, and Figure 6B). This indicated nearly complete bacterial eradication. HiPIMS sputtering for 60 sec resulted in a killing rate of 89.62% (Figure 6B), which, although lower than the 15 sec HiPIMS treatment, still outperformed both DCMS samples. These results highlight the critical role of sputtering technique and duration in determining the antibacterial efficacy of Au-ZnO NRs. HiPIMS-decorated samples consistently outperformed DCMS samples, likely due to the pulsed plasma's ability to deposit smaller, well-distributed Au nanoparticles, and the high energy from the HIPIMS power source enabled the Au nanoparticles to sputter onto the surface and adhere well to the ZnO NRs surface.[8]

To further elaborate on the advantages of HiPIMS over DCMS techniques, HiPIMS generates high peak power densities, resulting in the creation of plasma with a significantly higher ionization fraction compared to conventional DCMS. In HiPIMS, the plasma contains a larger proportion of ionized species (30-70%) than neutral atoms, enabling better energy transfer to the target material. Consequently, the ejected particles possessed higher kinetic energy, leading to the deposition of smaller, more uniformly distributed nanoparticles with strong adhesion to the ZnO nanorod surfaces. In contrast, DCMS produces a lower plasma density and a predominance of neutral atoms, resulting in the formation of larger nanoparticles with a less uniform distribution and weaker adhesion to the substrate. The smaller particle size and superior dispersion achieved by HiPIMS increased the surface area available for bacterial interactions and facilitated greater generation of reactive oxygen species (ROS) under UVA light exposure, thereby enhancing antibacterial efficacy. Furthermore, the stronger adhesion provided by the HiPIMS deposition ensures greater durability of the antibacterial coating during practical applications. These mechanisms collectively explain the superior antibacterial performance observed for the HiPIMS-Au 15sec/ZnO NRs compared to that of the DCMS-decorated samples. This observation is consistent with previous reports, which demonstrated that HiPIMS techniques yield denser, smoother, and more functional nanostructured films than DCMS approaches.[9,10,12,]

This significantly improves the performance, as the nanoparticles work synergistically with ZnO to enhance ROS generation under UV-A light and disrupt bacterial cell membranes through additional mechanisms, such as ion release. The superior performance of HiPIMS Au-ZnO NRs, particularly with a sputtering duration of 15 sec, underscores

their potential as effective antibacterial agents.[13] These findings suggest that optimizing sputtering conditions can n not only improve antibacterial efficacy, but also reduce material and production costs, making them suitable for applications in healthcare, water purification, and environmental remediation.

In this study, the antibacterial activity of samples exposed to UV-A was evaluated. Future studies should investigate the efficacy of these materials under other irradiation conditions. However, the experimental data demonstrated that the use of ZnO NRs, including those decorated with Au nanoparticles, via both DCMS and HiPIMS methods did not result in a significant reduction in *S. aureus* colonies (Supplementary data). Despite UV-A exposure, the nanorods did not effectively inhibit the growth of *S. aureus*. This suggests that the antibacterial properties observed in *E. coli* may not extend to *S. aureus* under the tested conditions, indicating a potential limitation in the effectiveness of Au-decorated ZnO NRs against this specific bacterial strain.[14]

These results indicated that additional modifications or alternative approaches may be necessary to achieve effective antibacterial activity against *S. aureus*. Future studies should explore the long-term stability and reusability of the HiPIMS-Au-ZnO NRs in real-world applications. Further investigation is warranted to examine the effects of Au nanoparticle size, shape, and distribution on antibacterial performance. Additionally, the development of scalable and cost-effective fabrication techniques for HiPIMS-decorated nanomaterials is recommended.

Limitation

This study was limited to *E. coli*. Expanding the scope to include other bacterial species, especially multi-drug-resistant strains, is essential.

Conclusion

The antibacterial efficacy of ZnO NRs decorated with Au nanoparticles was tested against *Escherichia coli have successfully achieved* at 10^6 CFU/mL under UVA exposure for 1 hr. Untreated controls showed dense bacterial growth. ASD-ZnO NRs displayed limited activity, with a killing rate of 26.64%. Au decoration via DCMS for 15 sec and 60 sec achieved moderate antibacterial effects (85.69% and 84.93% killing rates, respectively). HiPIMS for 15 sec showed the highest efficacy with a 99.62% killing rate, followed by HiPIMS for 60 sec at 89.62%.

These results highlight the enhanced antibacterial activity of Au-decorated ZnO NRs, especially with HiPIMS for 15 sec. Au decoration significantly enhanced the antibacterial efficacy of the ZnO NRs, with HiPIMS sputtering at 15 sec providing the highest performance. These results highlight the potential of Au-ZnO NRs as innovative solutions for combating bacterial infections, particularly in the context of antimicrobial resistance. Further studies should explore scalability, long-term stability, and efficacy against a broader spectrum of pathogens to facilitate their practical application.

Funding

This research received financial support from Bangkokthonburi University.

Conflict of interest

The authors declare that they have no conflicts of interest.

Credit authorship contribution statement

Sukon Kalasung: conceptualization, methodology, formal analysis, investigation, writing original draft, writing review and editing, visualization, validation; **Saksorn Limwichean:** conceptualization, methodology, investigation, validation, resources; **Pitak Eiamchai:** methodology, investigation, resources; **Mati Horprathum:** methodology, investigation, resources; **Noppadon Nuntawong:** methodology, investigation, resources; **Viyapol Patthanasettakul:** methodology, investigation, resources; **Artitaya Yatsomboon:** conceptualization, methodology, form alanalysis, investigation, writing review and editing, visualization, validation.

Acknowledgements

The authors would like to thank Bangkokthonburi University, National Electronics and Computer Technology Center (NECTEC), and National Science and Technology Development Agency (NSTDA) for their financial support through research.

References

[1] O'Neill J. Tackling drug-resistant infections globally: final report and recommendations. London: Wellcome Trust; 2016.

[2] Naghavi M, Vollset SE, Ikuta KS, Swetschinski LR, Gray AP, Wool EE, et al. Global burden of bacterial antimicrobial resistance 1990-2021: a systematic analysis with forecasts to 2050. The Lancet. 2024; 404(10459): 1199-226. doi: 10.1016/S0140-6736(24) 01867-1.

[3] Xie J, Li H, Zhang T, Song B, Wang X, Gu Z. Recent advances in ZnO nanomaterial-mediated biological applications and action mechanisms. Nanomaterials. 2023;13(9):1500. doi: 10.3390/nano13091500.

[4] Kalasung S, Aiempanakit K, Chatnuntawech I, Limsuwan N, Lertborworn K, Patthanasettakul V, et al. Trace-level detection and classifications of pentaerythritol tetranitrate via geometrically optimized film-based Au/ZnO SERS sensors. Sens Actuators B Chem. 2022; 366: 131986. doi: 10.1016/j. snb.2022.131986.

[5] Khan SS, Ullah I, Ullah S, An R, Xu H, Nie K, et al. Recent advances in the surface functionalization of nanomaterials for antimicrobial applications. Materials. 2021;14(22): 6932. doi: 10.3390/ma14226932.

[6] Nuchuay P, Laongwan C, Promcham W, Somboonsaksri P, Kalasung S, Chananonnawathorn C, et al. A study of the electrical and optical properties of AZO thin film by controlling pulse frequency of HiPIMS. J.Met. Mater.Miner.2023; 33(2): 103-7. doi: 10.55713/jmmm.

v33i2.1696.
[7] Sornsanit K, Horprathum M, Eiamchai P, Chananonnawathorn C, Kalasung S, Kaewkhao J. Enhanced antibacterial activity by Au nanoparticle decorated ZnO nanorods. Key Eng Mater. 2016;113–6.
[8] Dediu V, Busila M, Tucureanu V, Bucur FI, Iliescu FS, Brincoveanu O, et al. Synthesis of ZnO/Au Nanocomposite for Antibacterial Applications. Nanomaterials. 2022; 12(21): 3832 doi: 10.3390/nano12213832.
[9] Fageria P, Gangopadhyay S, Pande S. Synthesis of ZnO/Au and ZnO/Ag nanoparticles and their photocatalytic application using UV and visible light. RSC Adv. 2014; 4(48): 24962-72. doi: 10.1039/C4RA03158J.
[10] Kalasung S, Kopwitthaya A, Horprathum M, Kaewkhao J, Tuscharoen S, Eiamchai P, et al. Functionalization of Au nanoparticles on ZnO nanorods through low-temperature synthesis. Key Eng Mater. 2016; 675-6: 45-8. doi: 10.4028/www.scientific.net/KEM.675-676.45.
[11] Kalasung S, Chatnuntawech I, Patthanasettakul V, Limwichean S, Lertborworn K, Horprathum M, et al. Au-decorated ZnO nanorod arrays for SERS-active substrates towards trace detection and classification of pentaerythritol tetranitrate. Mater Today Proc. 2022; 56: 2245–2251. doi: 10.1016/j.matpr.2021.03.511
[12] Busila M, Musat V, Alexandru P, Romanitan C, Brincoveanu O, Tucureanu V, et al. Antibacterial and Photocatalytic Activity of ZnO/Au and ZnO/Ag Nanocomposites. Int J Mol Sci. 2023; 24(23): 16939 doi: 10.3390/ijms242316939
[13] Abebe B, Zereffa EA, Tadesse A, Murthy HCA. A Review on Enhancing the Antibacterial Activity of ZnO: Mechanisms and Microscopic Investigation, Nanoscale Res. Lett. 2020; 15: 190 doi: 10.1186/s11671-020-03418-6.
[14] Mlynarczyk-Bonikowska B, Kowalewski C, Krolak-Ulinska A, Marusza W. Molecular Mechanisms of Drug Resistance in *Staphylococcus aureus*. Int J Mol Sci. 2022 Jul 22; 23(15): 8088. doi: 10.3390/ijms23158088.

Supplementary Data

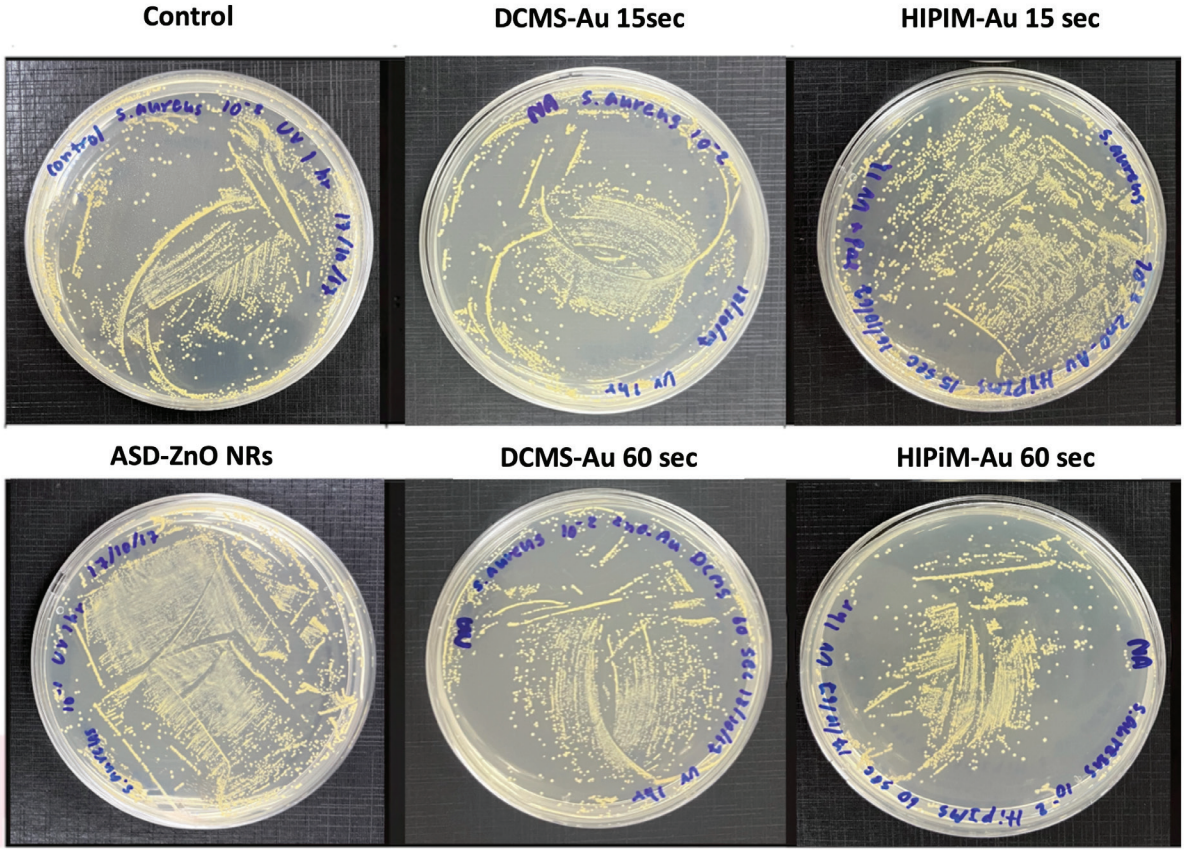

The antibacterial efficacy of ZnO nanorods (ZnO NRs) and gold-decorated ZnO nanorods (Au-ZnO NRs) was evaluated against *Staphylococcus aureus* at a concentration of 10^6 CFU/mL under UV-A exposure for 1 hr. The results showed no significant differences in antibacterial activity against *Staphylococcus aureus* among the control group, ZnO NRs, and Au-decorated ZnO NRs, regardless of the sputtering technique or duration.